CrossMark

U(VI) capture from aqueous solution by highly porous and stable MOFs: UiO-66 and its amine derivative

Bai-Cheng Luo[1,2] · Li-Yong Yuan[2] · Zhi-Fang Chai[2,3] · Wei-Qun Shi[2] · Quan Tang[1]

Abstract Metal–organic frameworks (MOFs) UiO-66 and its amine derivative (UiO-66-NH$_2$) with high surface area and unprecedented chemical stability were synthesized and first explored for U(VI) capture from aqueous solutions. At pH 5.5, U(VI) sorption reach equilibrium in ca. 4 h and the maximum sorption capacity is more than 100 mg g^{-1}. Moreover, they show desirable selectivity towards U(VI) over a range of competing metal ions. Sorption results demonstrate that introduction of amino groups into MOFs does not enhance U(VI) sorption, probably result from the lower activity of aromatic amines, decrease of surface area and formation of intermolecular hydrogen bonds.

Keywords Metal–organic frameworks · UiO-66 · Amine derivative · Uranium · Sorption

Introduction

Nuclear power industry has recently been rapidly developed, whereas the Fukushima nuclear accident has drawn much attention to develop a variety of technologies for the removal of radionuclides in nuclear fuel effluent, mine tailings, and other waste sources [1, 2]. On the other hand, uranium as the typical nuclear fuel, is radioactive and highly toxic [3]. Once the uranium enters into a human body, it will result in irreversible damage on internal organs [4]. Again, uranium source is in short supply for sustainable development of nuclear energy, thus require a reasonable and saving usage. All these issues promote the basic researches on fabrication of versatile materials for removal and recovery of uranium from the environment [5–8]. Metal–organic frameworks (MOFs), as a member of porous materials, allow varying pore size and functionalities systematically. MOFs have been applied in various fields including gas storage [9, 10], heterogeneous catalysis [11], separation [12], sense [13], drug delivery and biomedical imaging [14, 15]. Very recent efforts by several investigators have focused on the application of functionalized MOFs in separation, in particular, on the utility of these materials as solid phase sorbents for capture of toxic heavy metals Cd [16], Hg [17], and Pd [18] from environmental samples. U(VI) sorption by MOFs was also investigated, Lin et al., for example, reported the first application of UiO-68 in extracting actinide elements [19], Sun and Shi et al. used MOF-76 to probe and extract U(VI) from aqueous solution [20], Shi et al. applied amine-grafted MIL-101(Cr) in U(VI) sorption [21]. These works highlight the vast opportunities of MOFs in uptake and separation of U(VI) from aqueous solution.

It is understandable that stability in aqueous solution or acidic media is required for MOFs to serve as sorbent. Lillerud et al. firstly synthesized a zirconium (IV) dicarboxylate porous material named as UiO-66 [22], which is demonstrated to have high surface area and unprecedented chemical stability. The stability is derived from the highly

✉ Li-Yong Yuan
yuanly@ihep.ac.cn

✉ Quan Tang
tangquan528@sina.com

[1] School of Nuclear Science and Technology, University of South China, Hengyang 421001, China

[2] Laboratory of Nuclear Energy Chemistry, Institute of High Energy Physics, Chinese Academy of Sciences, Beijing 100049, China

[3] School of Radiological & Interdisciplinary Sciences, Soochow University, Suzhou 215123, China

oxophilic nature of zirconium (IV), the SBU (Zr_6-cluster) formed in the MOFs makes it very resistant towards various solvents and high temperature. The aperture (6 Å) is large enough to accommodate uranyl ions. Besides, a series of frameworks with structure based on the skeleton of UiO-66, e.g. UiO-66-NH$_2$, UiO-66-NO$_2$, and UiO-66-Br were also synthesized [23].

It is well known that amino group always serve as soft donors for actinides and have a better selectivity toward U(VI) over other metal ions. In this work, the UiO-66 and UiO-66-NH$_2$ were prepared and firstly explored for U(VI) capture from aqueous solution. The prepared UiO-66 and UiO-66-NH$_2$ were characterized by XRD, FT-IR, N$_2$ sorption and TGA. The effectiveness of these two MOFs for U(VI) sorption was assessed. The effect of various parameters such as contact time, pH, ion strength and initial U(VI) concentration on the sorption, as well as the selectivity of the sorbents for U(VI) were investigated in detail. This work promises to develop another simple and effective U(VI) sorbent for environmental remediation and extraction of uranium from seawater.

Experiment section

Materials

ZrCl$_4$ was purchased from Alfa Aesar. 1, 4-benzene dicarboxylic acid (H$_2$BDC) and 2-amine-benzenedicarboxylic acid (NH$_2$-H$_2$BDC) were purchased from Aladdin Ltd. (Shanghai, China). UO$_2$(NO$_3$)$_2$·6H$_2$O was purchased from Merck, Germany. All other chemicals obtained from Beijing Chemical Corp. were of analytical grade or better and used without further purification. Milli-Q-water (18.2 MΩ cm, Millipore Co.) was used in all experiments.

Preparation of isoreticular UiO-66

In a typical synthesis [24], terephthalic acid (0.233 mmol) along with ZrCl$_4$ (0.233 mmol) and DMF (3 mL) were placed in a 15 mL Teflon lined autoclave and heated at 120 °C for 24 h. After cooling, the microcrystalline precipitate was recovered by centrifugation. Residual DMF and terephthalic acid precursors still attached on UiO-66 were removed by reflux in DMF at 160 °C for 24 h, and washed by DMF (3 × 5 mL) and ethanol (3 × 5 mL). The product solid was finally dried overnight at 80 °C under air atmosphere. UiO-66-NH$_2$ was synthesized using the same strategy except that H$_2$N-H$_2$BDC instead of H$_2$BDC and additional 100 μL concentrated hydrochloric acid were used.

Characterizations of UiO-66 and UiO-66-NH$_2$

Power X-ray diffraction (PXRD) patterns of the materials were obtained on a Bruker D8-Advance X-ray Diffractometer with a Cu $K\alpha$ radiation ($\lambda = 1.5406$ Å) at a step size of 0.02°. Data of Fourier transform infrared spectra of the prepared samples were recorded on a Bruker Tensor 27 spectrometer with a potassium bromide pellet method. In order to study the thermal stability of the products, thermogravimetric curve was recorded on a thermal gravimetric analyzer (TGA, TA Instruments, Q500) from 20 to 800 °C by using a heating rate of 3 °C min^{-1} under N$_2$ flow. The N$_2$ sorption–desorption experiments were carried out at a liquid nitrogen temperature (−196 °C) using a micromeritics ASAP 2020 HD88 instrument with prior degassing under vacuum at 120 °C. The specific surface area was calculated by the Brunauer–Emmett–Teller method.

Batch sorption studies

All sorption experiments were carried out using a batch method in air at room temperature with initial concentrations of U(VI) ranging from 5 to 120 mg L^{-1}. Solution pH was measured on a digital pH-meter (Mettler Toledo) and adjusted using negligible volumes of HNO$_3$ or NaOH solutions. In a typical experiment, the sorbent (4.0 mg) was added into 10 mL solution containing U(VI) in a beaker, stirred for specified time (t, min), and then the solid phase was separated from the solution by using a 0.22 μm nylon membrane filter. The concentration of U(VI) in the supernatant was determined by Arsenazo III spectrophotometric method at wavelength of 656 nm (the detection limit of the method is below 0.1 ppm). Before the determination, the supernatant was diluted 50 times to make sure that the U(VI) concentration in the dilution is 0.1–5 μg mL^{-1}, corresponding to the UV absorbance of 0.05–1.0 at 656 nm. Samples containing uranium and other metal ions were acidified by 4 % analytical purity HNO$_3$, and the concentrations were analyzed by inductively coupled plasma optical emission spectrometer (ICP-OES, Horiba JY2000-2, Japan). The sorption capacity (q_e) for U(VI) was defined as follows:

$$q_e = \frac{(c_o - c_e) \times V}{m} \quad (1)$$

where c_0 and c_e are the initial and equilibrium concentrations of U(VI) (mg L^{-1}), respectively. V is the volume of the testing solution (mL), and m is the amount of sorbent (g). Experiments were performed in duplicates and the error bars associated with data shown in figures represent the standard deviations of the two runs.

Results and discussion

Characterizations of UiO-66 and UiO-66-NH$_2$

The characterization results of the two materials are shown in Fig. 1. The PXRD pattern of freshly prepared UiO-66 is consistent with that previously reported, indicating the successful formation of the material. The similar diffraction spectrum of UiO-66-NH$_2$ with that of UiO-66 is an indication that the tagged UiO-66-NH$_2$ is topologically equivalent with UiO-66. After U(VI) sorption, PXRD patterns keeps unchanged,which reveals the preservation of the MOFs skeleton during U(VI) sorption. Figure 1b represents the FTIR spectra of the two materials, two absorption bands at 3405 and 3362 cm^{-1} can be discerned, corresponding to the asymmetric and symmetric N–H stretching modes, respectively. The C–N stretching vibration of UiO-66-NH$_2$ is revealed at 1255 cm^{-1}. After U(VI) sorption, the absorption at 900 cm^{-1} assigned to the v_{as} stretching vibration of O=U=O appeared. Figure 1c shows TGA profiles of the two materials. For UiO-66, the most significant weight loss points appear at temperature above 450 °C, corresponding to the collapse of the MOF skeleton. Whereas for UiO-66-NH$_2$, this temperature decreased to 300 °C due to the introduction of amino group. Whatever, the TGA profiles suggest that the prepared MOFs have excellent thermal stability. The BET specific surface areas of UiO-66 and UiO-66-NH$_2$ were determined to be 1382 and 1050 m^2 g^{-1}, respectively, showing the ultra-high surface area of these materials. And the pore volumes of UiO-66 and UiO-66-NH$_2$ are 0.55 and 0.36 cm^3 g^{-1}, respectively. These data confirm the successful preparation of amino-grafted UiO-66 and that the introduction of amino-group obviously decrease the surface area and pore volume of UiO-66.
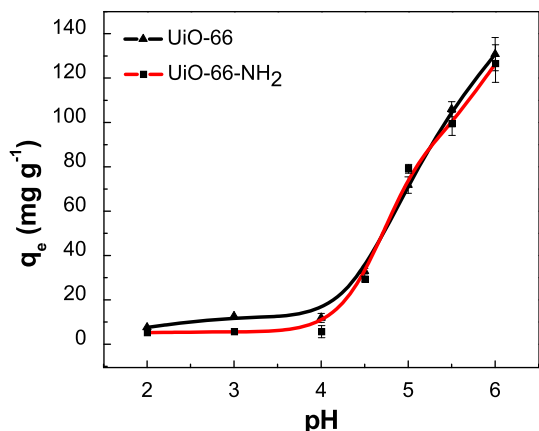
U (VI) sorption by UiO-66 and UiO-66-NH$_2$

Effect of pH

U(VI) sorption UiO-66 and UiO-66-NH$_2$ were performed at different pH values ranging from 2.0 to 6.0 to assess the effect of solution pH on the sorption. The results are given in Fig. 2. It was found that UiO-66 and UiO-66-NH$_2$ shows similar pH-dependent U(VI) sorption. That is, the sorption capacity remained very low at pH from 2.0 to 4.0 and increased sharply thereafter. When pH reached 5.5, the sorption capacity for both sorbents was more than 100 mg g^{-1}. Similar pH-dependent sorption were observed when applying amino [25] and imidazole groups [26] functionalized SBA-15 in the removal of U(VI) and in the case of amidoxime modified mesoporous carbon as U(VI) sorbent [27]. Such a pH-dependent sorption may be

Fig. 1 Characterization of UiO-66 *1*, U(VI)-loaded UiO-66 *2*, UiO-66-NH$_2$ *3* and U(VI)-loaded UiO-66-NH$_2$ *4*. **a** PXRD patterns; **b** FTIR spectra; **c** TGA profiles; **d** N$_2$ sorption/desorption isotherms
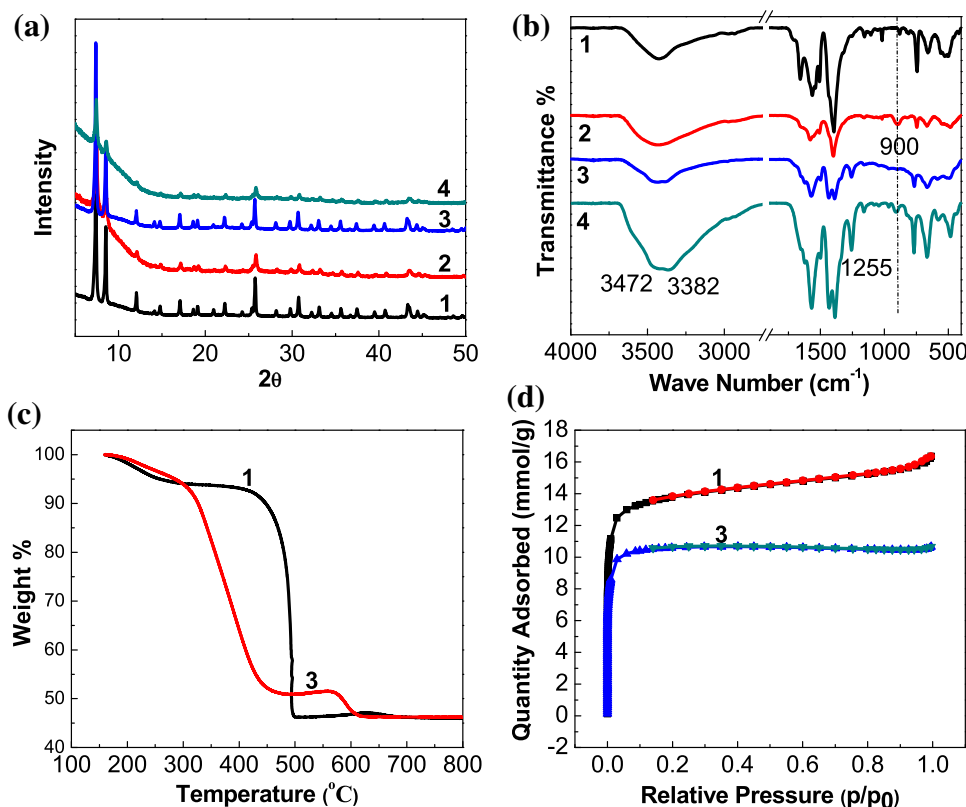
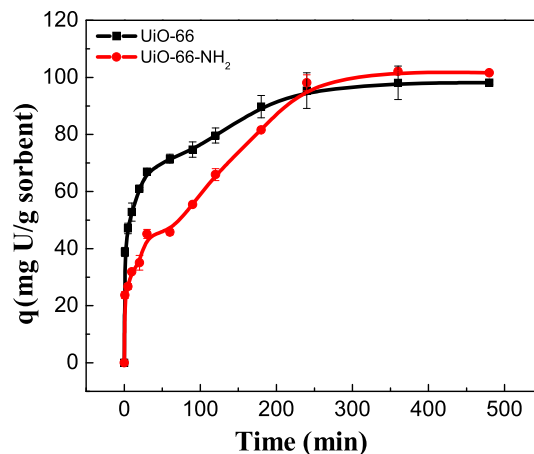**Fig. 2** Effect of pH on the sorption of U(VI) onto UiO-66 and UiO-66-NH$_2$; $t = 240$ min, $m_{sorbent} = 4.0$ mg, $V_{solution} = 10$ mL, $c_0 = 100$ mg L^{-1}, $T = 14$ °C

Fig. 3 Effect of contact time on the sorption of U(VI) onto UiO-66 and UiO-66-NH$_2$. pH 5.5 ± 0.1, $m_{sorbent} = 4.0$ mg, $V_{solution} = 10$ mL, $c_0 = 100$ mg L^{-1}, and $T = 14$ °C

rationalized based on the surface charge of the sorbents. At lower pH, the active sites on the sorbents are protonated and positively charged. The positively charged U(VI) ions are not favored by the positively charged active sites due to the electrostatic repulsion effect, leading to a lower sorption capacity. As pH increases, the active sites become deprotonated, and the electrostatic repulsion between the binding groups and U(VI) ions diminishes and even disappears. The coordination or hydrogen bonds interaction incites an increase of the sorption capacity. On the other hand, pH-induced U(VI) speciation may also be responsible for the pH-dependent sorption. It is well known that with the increasing of pH, U(VI) species transform gradually from free UO$_2^{2+}$ to multi-nuclear hydroxide complexes such as (UO$_2^{2+}$)$_3$(OH)$_5^+$ [26]. These hydroxide complexes may be more favored by the sorbents. In the following experiments, pH 5.5 ± 0.1 was selected as the appropriate condition for further investigation.

Effect of contact time

The U(VI) sorption on UiO-66 and UiO-66-NH$_2$ for U(VI) as a function of contact time were shown in Fig. 3. The U(VI) sorption on UiO-66 increased rapidly during the first 1 h and then gradually reached an equilibrium. For UiO-66-NH$_2$, the sorption kinetics is slower requiring about 4 h to reach the equilibrium. The decreased surface area and pore volume of UiO-66-NH$_2$ compared with UiO-66 might be responsible for the slower sorption. It probably took longer time for U(VI) ions to diffuse into the pore structure of UiO-66-NH$_2$ and sorb onto the surface.

Two kinetic models, i.e. pseudo-first-order and pseudo-second-order models were employed to describe the sorption process. The linear form of the two models can be expressed as follows:.

The pseudo-first-order Eq. (2):

$$\ln(q_e - q_t) = \ln q_e - k_1 t \tag{2}$$

The pseudo-second-order Eq. (3):

$$\frac{t}{q_t} = \frac{1}{k_2 q_e^2} + \frac{t}{q_e} \tag{3}$$

where q_t and q_e are the amounts of U(VI) ions adsorbed (mg g^{-1}) at time t (min) and equilibrium, respectively; k_1 (min^{-1}) and k_2 (g mg^{-1} min^{-1}) are the pseudo-first-order and the pseudo-second-order sorption rate constants, respectively. The kinetics data for both sorbents were fitted by the two kinetics models and the parameters obtained from the fitting are listed in Table 1. From the results it can be seen that both pseudo-first and pseudo-second order models reasonably match with the experimental kinetics data for the both sorbents. However, the pseudo-second order model gives much better correlation coefficient (>0.99 for UiO-66 and >0.96 for UiO-66-NH$_2$) and much closer the sorption capacity (q_e) to the experimentally observed equilibrium capacity, suggesting that the pseudo-second order model is more appropriate to explain the kinetics of U(VI) sorption onto the both sorbents. This result gives a hint that the U(VI) sorption rate onto UiO-66 and UiO-66-NH$_2$ is mainly controlled by the chemical reactions between U(VI) and sorption site of the sorbents, the U(VI) ions diffusion, however, also plays important role on the rate determination.

Sorption isotherm

Equilibrium isotherm studies were carried out to evaluate the maximum sorption capacity for U(VI), on UiO-66 and UiO-66-NH$_2$ in which the initial concentrations of U(VI) were varied from 5 to 120 mg L^{-1} and the solution pH was

Table 1 Kinetics model constants and correlation coefficients for U(VI) sorption by UiO-66 and UiO-66-NH$_2$

|	Pseudo-first-order			Pseudo-second-order		
	q_e (mg g^{-1})	k_1 (min^{-1})	R^2	q_e (mg g^{-1})	k_2 (g mg^{-1} min^{-1})	R^2
UiO-66	50.2	0.0095	0.965	101.0	0.0015	0.996
UiO-66-NH$_2$	87.2	0.0100	0.923	109.9	0.0037	0.966

kept at 5.5 ± 0.1. The amount of sorbed U(VI) as a function of equilibrium U(VI) concentration in aqueous phase (C_e) was shown in Fig. 4. It can be seen that the sorption capacity for U(VI) onto the UiO-66 and UiO-66-NH$_2$ increased gradually with the increase of the initial U(VI) concentration and finally attained saturation sorption. Besides, the comparison shows that there is no significant difference in U(VI) sorption on UiO-66 and UiO-66-NH$_2$.

The sorption data were applied to Langmuir and Freundlich isotherm models to understand the sorption mechanism. The Langmuir and Freundlich models are expressed as Eqs. (4) and (5), respectively:

$$\frac{c_e}{q_e} = \frac{1}{bq_m} + \frac{c_e}{q_m} \tag{4}$$

$$\ln q_e = \ln K_F - \frac{1}{n} \ln c_e \tag{5}$$

where q_e (mg g^{-1}) and c_e (mg L^{-1}) are the amount of sorbed adsorbate on the sorbent and the concentration of adsorbate in the solution at equilibrium time, respectively. The b (L mg^{-1}) and K_F are the Langmuir and Freundlich sorption isotherm model coefficient. The b is the constant related to the free energy of adsorption and represents the affinity of adsorbate and adsorbent, and the K_F is the constant indicative of the relative adsorption capacity of the absorbent (mg g^{-1}), respectively. The isotherm parameters calculated from the fitting are shown in Table 2. It
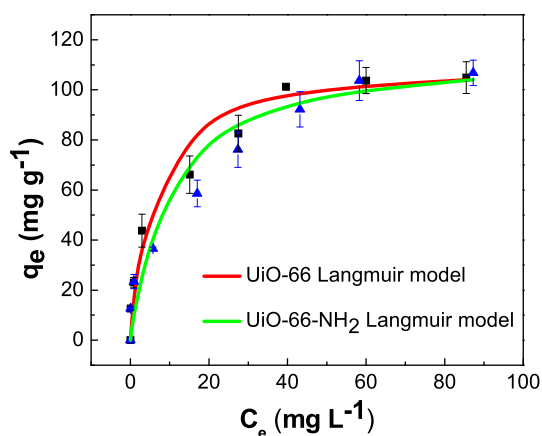
is concluded from the higher correlation coefficients ($R^2 \geq 0.97$) that the Langmuir equation fits the data better than the Freundlich model for both UiO-66 and UiO-66-NH$_2$ from which the maximum sorption capacity of UiO-66 and UiO-66-NH$_2$ was evaluated as 109.9 and 114.9 mg g^{-1}, respectively. The Langmuir model indicates that the sorbed U(VI) is uniformly distributed in a monolayer coverage of the surface of the sorbents.

In order to further understand the sorption mechanism, the Dubinin–Raduseckevich (D-R) isotherm was applied to the sorption data to obtain the sorption free energy E. E could be obtained by following formulas:

$$\ln q_e = \ln Q_m - \beta \varepsilon^2 \tag{6}$$

$$\varepsilon = RT \ln\left(1 + \frac{1}{C_e}\right) \tag{7}$$

$$E = (2\beta)^{-0.5} \tag{8}$$

where Q_m (mol g^{-1}) represents theoretical monolayer saturation capacity; β (mol^2 kJ^{-2}) is a constant correlated to sorption energy. ε is Polanyi potential (kJ mol^{-1}) related to the equilibrium concentration. R is the universal gas constant [kJ (mol K)$^{-1}$] and T is the absolute temperature (K). By fitting the sorption data, The E values were evaluated to be 14.7 and 14.2 kJ mol^{-1} for UiO-66 and UiO-66-NH$_2$, respectively. It is deemed that the E value located in the range of 1–8 kJ mol^{-1} indicates that the sorption process is dominated by physical sorption, while the value located at 9–16 kJ mol^{-1} implies that chemical sorption is prominent. Therefore, it was concluded that U(VI) sorption on both UiO-66 and UiO-66-NH$_2$ is of chemical sorption mechanism.

Effect of ionic strength

The effect of ionic strength on the U(VI) sorption on UiO-66 and UiO-66-NH$_2$ was studied in the presence of NaClO$_4$ with concentrations varied from 10^{-4} to 10^{-1} mol L^{-1}. This test is of great importance on account of assessing the feasibility of a solid sorbent applied in the removal or recovery of U(VI) from wastewater with different concentration salts. The results are shown in Fig. 5, it can be seen that the U(VI) sorption on both UiO-66 and UiO-66-NH$_2$ did not change significantly with the increase of the ionic strength (even at the NaClO$_4$ concentration more than 0.1 mol L^{-1}). The results are interesting and important,

Fig. 4 Effect of the initial U(VI) concentration on U(VI) sorption onto UiO-66 and UiO-66-NH$_2$. pH 5.5 ± 0.1, $t = 240$ min, $m_{\text{sorbent}} = 4.0$ mg, $V_{\text{solution}} = 10$ mL and $T = 14$ °C

Table 2 Isotherm model parameters for U(VI) sorption by UiO-66 and UiO-66-NH$_2$

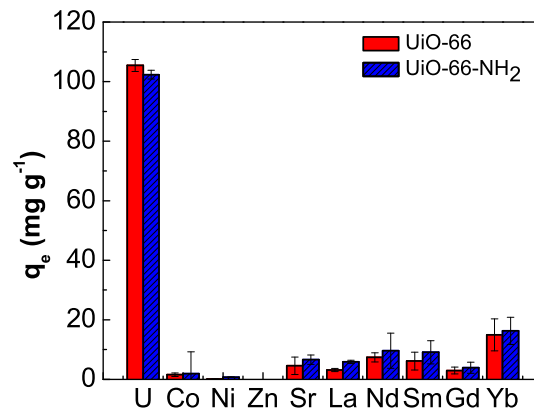|	Langmuir			Freundlich		
	q_m (mg g^{-1})	b (L mg^{-1})	R^2	K_F (mg g^{-1})	n	R^2
UiO-66	109.9	0.21	0.99	29.3	3.26	0.98
UiO-66-NH$_2$	114.9	0.12	0.97	25.1	3.07	0.96
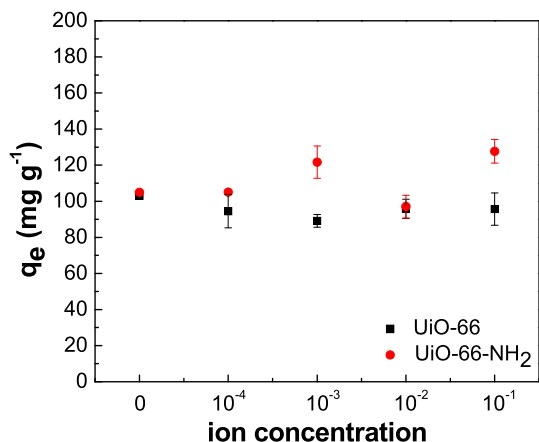
Fig. 5 Effect of ion strength on the U(VI) sorption by UiO-66 and UiO-66-NH$_2$; pH 5.5 ± 0.1, t = 240 min, $m_{sorbent}$ = 4.0 mg, $V_{solution}$ = 10 mL, and T = 14 °C

Fig. 6 Competitive sorption of coexistent ions at pH 5.5 ± 0.1. The initial concentration of all metal ions was 0.5 mmol L^{-1}

and are very different from that on functionalized mesoporous silica, in which U(VI) sorption decreased significantly with the increase of NaClO$_4$ concentration [28]. It is well known that the salt concentration is very high in wastewater or seawater. The independent ionic strength sorption of U(VI) on the MOFs at high salt concentrations is critical for the application of MOFs in wastewater cleaning or recovery of U(VI) from seawater.

Selectivity test

The selectivity is another significant property for the practical application of the materials. U(VI) sorption by UiO-66 and UiO-66-NH$_2$ from the mimic waste water containing various metal ions, including Zn^{2+}, Co^{2+}, Ni^{2+}, Sr^{2+}, Cr^{3+}, La^{3+}, Ce^{3+}, Yb^{3+} and Nd^{3+}, was examined at pH 5.5 ± 0.1, to evaluate the selectivity of UiO-66 series materials for U(VI). The result is shown in Fig. 6. It can be seen that the uptake of U(VI) on UiO-66 and UiO-66-NH$_2$ is as high as 108 and 104 mg g^{-1}, respectively, while that of all other metal ions is less than 20 mg g^{-1}.

It was clear that the competing ions used in the present study have almost no significant influence on the uptake of U(VI) by UiO-66 and UiO-66-NH$_2$ under the experimental conditions used. The result of the selectivity test exhibits the following affinity sequence: U(VI) > Yb^{3+} > Nd^{3+} > Sm^{3+} > Sr^{2+} > La^{3+} > Gd^{3+} > Co^{2+} > Ni^{2+} > Zn^{2+} for UiO-66 and UiO-66-NH$_2$. The results, on the one hand, suggest that both UiO-66 and UiO-66-NH$_2$ sorbents

shows a desirable selectivity for U(VI) ions over a range of competing metal ions. On the other hand, it is further confirmed that ionic strength has negligible effects on the U(VI) sorption by the MOFs sorbent.

Comparison and understanding of U(VI) sorption by UiO-66 and UiO-66-NH$_2$

From our previous published works [21, 26, 29, 30], it is concluded that amino group always serve as soft donors for actinides and have a better selectivity toward U(VI) over other metal ions. In this work, however, there was no significant improvement for the U(VI) on UiO-66 after introduction of amino group. This probably can be rationalized from the following aspects: (1) Aromatic amines are always less active for binding metal ions than aliphatic amine, which maybe result from the steric hindrance of aromatic rings. (2) It is can be seen from the Fig. 1b that a peak split at ∼1400 cm^{-1} is a favorable evidence of intermolecular hydrogen bond occurring between carboxyl and amino groups in the UiO-66-NH$_2$. (3) The introduction of amino group aroused the decrease of surface area (from 1382 to 1050 m^2 g^{-1}) and pore volume (from 0.55 to 0.36 cm^3 g^{-1}) of UiO-66. All above issues could be responsible for the comparable U(VI) sorption by UiO-66 and its amine derivative.

Besides, the U(VI) sorption results from this work were also compared with those for other previous reported MOFs such as UiO-68, MOF-76 and MIL-101 series, as

Table 3 A summary of U(VI) uptake by UiO-66 and its amine derivative, as well as by other MOFs previously reported

Samples	Saturation capacity (mg g^{-1})	BET surface area (m^2 g^{-1})	Pore volume (cm^3 g^{-1})
UiO-66	109.9	1382	0.55
UiO-66-NH$_2$	114.9	1050	0.36
MIL-101 [21]	20	3065	1.437
MIL-101-NH$_2$ [21]	90	1645	0.779
MIL-101-ED [21]	200	753	0.363
MIL-101-DETA [21]	350	1074	0.528
MOF-76 [20]	300[a]	NM	NM
UiO-68 [19]	217[b]	1350	65.7 %[c]

[a] Value obtained at pH 3.0 but decreased to 100 at pH 5.5

[b] Value obtained at pH 2.5 but decreased to 152 at pH 5.0

[c] Solvent accessible volume calculated with PLATON

NM not measured

shown in Table 3. It is found that the sorption capacities for UiO-66 and UiO-66-NH$_2$ are larger than MIL-101 and MIL-101-NH$_2$, but much lower than MIL-101-ED, MIL-101-DETA, UiO-68 and MOF-76. However, UiO-66 and UiO-66-NH$_2$ were prepared by a simple solvothermal method in one step, using commonly used reagents. That is, the preparation of UiO-66 and UiO-66-NH$_2$ is simple and low-cost unlike other functionalized MOFs. From this point of view, UiO-66 and UiO-66-NH$_2$ will be promising and applicable as effective sorbents for U(VI) removal from waste water and/or U(VI) enrichment from seawater.

Conclusions

UiO-66 and UiO-66-NH$_2$ were prepared by a simple solvothermal method using commonly used reagents and were used as an efficient U(VI) sorbent from aqueous solution. The efficiency was demonstrated by the fast sorption kinetics, large sorption capacity, ionic strength-independence, and a desirable selectivity towards U(VI) over a range of competing metal ions. However, the present results suggested that the U(VI) sorption could not be enhanced by introduction of amino group into UiO-66, probably due to the lower activity of aromatic amines, decrease of surface area and formation of intermolecular hydrogen bonds. This work provides new data for assessing the feasibility of this MOFs applied in separation of U(VI) from waste water and enrichment of U(VI) from seawater.

References

1. Rao TP, Metilda P, Gladis JM (2006) Preconcentration techniques for uranium(VI) and thorium(IV) prior to analytical determination-an overview. Talanta 68:1047–1064
2. Shi WQ, Zhao YL, Chai ZF (2012) Nuclear and radiochemistry in China: present status and future perspectives. Radiochim Acta 100:529–539
3. Yan S, Hua B, Bao Z, Yang J, Liu C, Deng B (2010) Uranium (VI) removal by nanoscale zerovalent iron in anoxic batch systems. Environ Sci Technol 44:7783–7789
4. Preetha CR, Gladis JM, Rao TP, Venkateswaran G (2006) Removal of toxic uranium from synthetic nuclear power reactor effluents using uranyl ion imprinted polymer particles. Environ Sci Technol 40:3070–3074
5. Metilda P, Mary Gladis J, Prasada Rao T (2004) Influence of binary/ternary complex of imprint ion on the preconcentration of uranium (VI) using ion imprinted polymer materials. Anal Chim Acta 512:63–73
6. Shi WQ, Yuan LY, Wang CZ, Wang L, Mei L, Xiao CL, Zhang L, Li ZJ, Zhao YL, Chai ZF (2014) Exploring actinide materials through synchrotron radiation techniques. Adv Mater 26:7807–7848
7. Shamsipur M, Fasihi J, Ashtari K (2007) Grafting of ion-imprinted polymers on the surface of silica gel particles through covalently surface-bound initiators: a selective sorbent for uranyl ion. Anal Chem 79:7116–7123
8. James D, Venkateswaran G, Prasada Rao T (2009) Removal of uranium from mining industry feed simulant solutions using trapped amidoxime functionality within a mesoporous imprinted polymer material. Microporous Mesoporous Mater 119:165–170
9. Ma S, Zhou H (2010) Gas storage in porous metal–organic frameworks for clean energy applications. Chem Commun 46:44–53
10. Murray LJ, Dincă M, Long JR (2009) Hydrogen storage in metal–organic frameworks. Chem Soc Rev 38:1294–1314
11. Yoon M, Srirambalaji R, Kim K (2011) Homochiral metal–organic frameworks for asymmetric heterogeneous catalysis. Chem Rev 112:1196–1231
12. Li J, Sculley J, Zhou H (2011) Metal–organic frameworks for separations. Chem Rev 112:869–932
13. Cui Y, Yue Y, Qian G, Chen B (2011) Luminescent functional metal–organic frameworks. Chem Rev 112:1126–1162
14. Horcajada P, Gref R, Baati T, Allan PK, Maurin G, Couvreur P, Férey G, Morris RE, Serre C (2011) Metal–organic frameworks in biomedicine. Chem Rev 112:1232–1268
15. Della Rocca J, Liu D, Lin W (2011) Nanoscale metal–organic frameworks for biomedical imaging and drug delivery. Acc Chem Res 44:957–968
16. Fang Q, Yuan D, Sculley J, Li J, Han Z, Zhou H (2010) Functional mesoporous metal–organic frameworks for the capture of heavy metal ions and size-selective catalysis. Inorg Chem 49:11637–11642
17. Zhou XP, Xu Z, Zeller M, Hunter AD (2009) Reversible uptake of HgCl$_2$ in a porous coordination polymer based on the dual functions of carboxylate and thioether. Chem Commun 36:5439–5441
18. Bagheri A, Taghizadeh M, Behbahani M, Akbar Asgharinezhad A, Salarian M, Dehghani A, Ebrahimzadeh H, Amini MM (2012) Synthesis and characterization of magnetic metal-organic

framework (MOF) as a novel sorbent, and its optimization by experimental design methodology for determination of palladium in environmental samples. Talanta 99:132–139

19. Carboni M, Abney CW, Liu S, Lin W (2013) Highly porous and stable metal–organic frameworks for uranium extraction. Chem Sci 4:2396

20. Yang W, Bai ZQ, Shi WQ, Yuan LY, Tian T, Chai ZF, Wang H, Sun ZM (2013) MOF-76: from a luminescent probe to highly efficient U(VI) sorption material. Chem Commun 49:10415–10417

21. Bai ZQ, Yuan LY, Zhu L, Liu ZR, Chu SQ, Zheng LR, Zhang J, Chai ZF, Shi WQ (2015) Introduction of amino groups into acid-resistant MOFs for enhanced U (vi) sorption. J Mater Chem A 3

22. Cavka JH, Jakobsen S, Olsbye U, Guillou N, Lamberti C, Bordiga S, Lillerud KP (2008) A new zirconium inorganic building brick forming metal organic frameworks with exceptional stability. J Am Chem Soc 130:13850–13851

23. Kandiah M, Nilsen MH, Usseglio S, Jakobsen S, Olsbye U, Tilset M, Larabi C, Quadrelli EA, Bonino F, Lillerud KP (2010) Synthesis and stability of tagged UiO-66 Zr-MOFs. Chem Mater 22:6632–6640

24. Garibay SJ, Cohen SM (2010) Isoreticular synthesis and modification of frameworks with the UiO-66 topology. Chem Commun (Camb) 46:7700–7702

25. Wang YL, Song LJ, Zhu L, Guo BL, Chen SW, Wu WS (2014) Removal of uranium(VI) from aqueous solution using iminodiacetic acid derivative functionalized SBA-15 as adsorbents. Dalton Trans 43:3739–3749

26. Yuan LY, Liu YL, Shi WQ, Zj Li, Lan JH, Feng YX, Zhao YL, Yuan YL, Chai ZF (2012) A novel mesoporous material for uranium extraction, dihydroimidazole functionalized SBA-15. J Mater Chem 22:17019–17026

27. Tian G, Geng J, Jin Y, Wang C, Li S, Chen Z, Wang H, Zhao Y, Li S (2011) Sorption of uranium (VI) using oxime-grafted ordered mesoporous carbon CMK-5. J Hazard Mater 190:442–450

28. Yuan LY, Liu YL, Shi WQ, Lv YL, Lan JH, Zhao YL, Chai ZF (2011) High performance of phosphonate-functionalized mesoporous silica for u(vi) sorption from aqueous solution. Dalton Trans 40:7446–7453

29. Wang XL, Yuan LY, Wang YF, Li ZJ, Lan JH, Liu YL, Feng YX, Zhao YL, Chai ZF, Shi WQ (2012) Mesoporous silica SBA-15 functionalized with phosphonate and amino groups for uranium uptake. Sci China Chem 55:1705–1711

30. Liu YL, Yuan LY, Yuan YL, Lan JH, Li ZJ, Feng YX, Zhao YL, Chai ZF, Shi WQ (2012) A high efficient sorption of U (VI) from aqueous solution using amino-functionalized SBA-15. J Radioanal Nucl Ch 292:803–810